

Supplementary Materials

Contents	Pages
Supplementary Text.....	2-4
Supplementary Tables.....	5-6
Supplementary Movies Legends.....	7
Supplementary Figures.....	8-12
Model Source Files.....	(8 appended files)

Supplementary Text

Computational model of the p53 response to UV

We generated a model of the p53 response to UV (UV_model.m and command_UV_model.m) based on our previously published model of the response to double strand breaks (DSBs) (Batchelor et al., 2008) using similar species and parameter values. We included new terms in the DSB model (DSB_model.m and command_DSB_model.m) to account for the dephosphorylation of active p53 by Wip1 (Lu et al., 2005). Since Mdm2-mediated ubiquitination of p53 is the dominant factor governing p53 degradation, we approximated the parameter governing the Wip1-mediated dephosphorylation of p53 to be one-tenth the value for the parameter governing Mdm2-mediated p53 degradation. The addition of these terms did not qualitatively alter the oscillatory behavior of p53 in the DSB model (Figure 2C of the main text and (Batchelor et al., 2008)). To construct the UV model, we eliminated the term in the DSB model describing the interaction between Wip1 and the upstream kinase, ATM (Figure 2A-B, main text). We have also reduced the strength of the ATR/Mdm2 interaction term to account for the fact that while phosphorylation of Mdm2 by ATM affects both Mdm2 activity and stability, phosphorylation of Mdm2 by ATR affects only Mdm2 activity (Stommel and Wahl, 2004 and main text). This resulted in the following set of delay differential equations describing the UV response:

$$\begin{aligned}\frac{d[p53_{inactive}]}{dt} &= \beta_p - \alpha_{mpi}[Mdm2][p53_{inactive}] - \beta_{sp}[p53_{inactive}] \frac{[ATR_{active}]^{n_s}}{[ATR_{active}]^{n_s} + T_s^{n_s}} \\ &+ \alpha_{wpa}[Wip1][p53_{active}] - \alpha_{pi}[p53_{inactive}] \\ \frac{d[p53_{active}]}{dt} &= \beta_{sp}[p53_{inactive}] \frac{[ATR_{active}]^{n_s}}{[ATR_{active}]^{n_s} + T_s^{n_s}} - \alpha_{mpa}[Mdm2][p53_{active}] - \alpha_{wpa}[Wip1][p53_{active}] \\ \frac{d[Mdm2]}{dt} &= \beta_m[p53_{active}(t - \tau_m)] + \beta_{mi} - \alpha_{sm2}[ATR_{active}][Mdm2] - \alpha_m[Mdm2] \\ \frac{d[Wip1]}{dt} &= \beta_w[p53_{active}(t - \tau_w)] - \alpha_w[Wip1] \\ \frac{d[ATR_{active}]}{dt} &= \beta_{s2}[\theta(t) - \theta(t - t_r)] - \alpha_s[ATR_{active}]\end{aligned}$$

Parameter values are listed in Supplementary Table 1. All numerical simulations were performed in Matlab using *dde23*. Values for the production rate of active ATR, β_{s2} , and the duration of active ATR signaling, t_r , for each modeled UV dose are listed in Supplementary Table 2.

Computational model of cross-talk between the ATM and ATR pathways

We generated a combined model to explore the possible contributions of cross-talk between the UV/ATR and the gamma/ATM pathways (DSB_crosstalk_model.m, command_DSB_crosstalk_model.m, UV_crosstalk_model.m, and command_UV_crosstalk_model.m) (Jazayeri et al., 2006)(Yajima et al., 2009). This resulted in the following set of differential equations:

$$\begin{aligned} \frac{d[p53_{inactive}]}{dt} &= \beta_p - \alpha_{mpi}[Mdm2][p53_{inactive}] - \beta_{sp}[p53_{inactive}] \left(\frac{[ATM - P]^{n_s}}{[ATM - P]^{n_s} + T_s^{n_s}} + \frac{[ATR_{active}]^{n_s}}{[ATR_{active}]^{n_s} + T_s^{n_s}} \right) \\ &+ \alpha_{wpa}[Wip1][p53_{active}] - \alpha_{pi}[p53_{inactive}] \\ \frac{d[p53_{active}]}{dt} &= \beta_{sp}[p53_{inactive}] \left(\frac{[ATM - P]^{n_s}}{[ATM - P]^{n_s} + T_s^{n_s}} + \frac{[ATR_{active}]^{n_s}}{[ATR_{active}]^{n_s} + T_s^{n_s}} \right) - \alpha_{mpa}[Mdm2][p53_{active}] - \alpha_{wpa}[Wip1][p53_{active}] \\ \frac{d[Mdm2]}{dt} &= \beta_m[p53_{active}(t - \tau_m)] + \beta_{mi} - \alpha_{sm}[ATM - P][Mdm2] - \alpha_{sm2}[ATR_{active}][Mdm2] - \alpha_m[Mdm2] \\ \frac{d[Wip1]}{dt} &= \beta_w[p53_{active}(t - \tau_w)] - \alpha_w[Wip1] \\ \frac{d[ATM - P]}{dt} &= \beta_s[\theta(t) - \theta(t - t_r)] - \alpha_{ws} \frac{[Wip1]^{n_w}}{[Wip1]^{n_w} + T_w^{n_w}} [ATM - P] - \alpha_s[ATM - P] \\ \frac{d[ATR_{active}]}{dt} &= \beta_{s2}[\theta(t) - \theta(t - t_r)] - \alpha_s[ATR_{active}] \end{aligned}$$

We used values of $\alpha_{ws} = 50 \text{ h}^{-1}$, $T_w = 0.2 \text{ C}_s$, and $n_w = 4$, as were used in the previously published model for the response to DSBs (Batchelor et al., 2008).

To estimate the amount of cross-talk between the signaling kinases, we measured the levels of Chk1 phosphorylated on Ser-317 and Chk2 phosphorylated on Thr-68, targets of ATR and ATM, respectively (Matsuoka et al., 2000; Zhao and Piwnica-Worms, 2001), in response to γ or UV irradiation (Figure 2G-H, Main Text). The ratio of maximum phospho-Chk1(S317) levels in response to γ compared with its levels in response to UV was 0.135. Therefore, to model the cross-talk of ATR in response to γ we

set $\beta_{s,DSB} = 0.135 * \beta_{s,UV}$. Similarly, the ratio of maximum phospho-Chk2(T68) levels in response to UV compared with its levels in response to γ was 0.108. Therefore, to model the cross-talk of ATM in response to UV we set $\beta_{s,UV} = 0.108 * \beta_{s,DSB}$. In response to DSBs, we used $\beta_s = 10 C_s h^{-1}$ (Batchelor et al, 2008). Simulation of the models indicated that there was minimal difference in p53 dynamics between models including or excluding the cross-talk in response to either γ or UV (Supplementary Figure 3; compare A to B and C to D).

Supplementary References

Batchelor, E., Mock, C.S., Bhan, I., Loewer, A., and Lahav, G. (2008). Recurrent initiation: a mechanism for triggering p53 pulses in response to DNA damage. *Mol Cell* 30, 277-289.

Jazayeri, A., Falck, J., Lukas, C., Bartek, J., Smith, G.C., Lukas, J., and Jackson, S.P. (2006). ATM- and cell cycle-dependent regulation of ATR in response to DNA double-strand breaks. *Nat Cell Biol* 8, 37-45.

Lu, X., Nannenga, B., and Donehower, L.A. (2005). PPM1D dephosphorylates Chk1 and p53 and abrogates cell cycle checkpoints. *Genes Dev* 19, 1162-1174.

Matsuoka, S., Rotman, G., Ogawa, A., Shiloh, Y., Tamai, K., and Elledge, S.J. (2000). Ataxia telangiectasia-mutated phosphorylates Chk2 in vivo and in vitro. *Proc Natl Acad Sci U S A* 97, 10389-10394.

Yajima, H., Lee, K.J., Zhang, S., Kobayashi, J., and Chen, B.P. (2009). DNA double-strand break formation upon UV-induced replication stress activates ATM and DNA-PKcs kinases. *J Mol Biol* 385, 800-810.

Zhao, H., and Piwnicka-Worms, H. (2001). ATR-mediated checkpoint pathways regulate phosphorylation and activation of human Chk1. *Mol Cell Biol* 21, 4129-4139.

Parameter	Description	Value
β_p	p53 _{inactive} production rate	$0.9 C_s h^{-1}$
β_{sp}	Saturating production rate of p53 _{active}	$10 h^{-1}$
β_m	p53-dependent Mdm2 production rate	$0.9 h^{-1}$
β_{mi}	p53-independent Mdm2 production rate	$0.2 C_s h^{-1}$
β_w	Wip1 production rate	$0.25 h^{-1}$
α_{mpi}	Mdm2-dependent p53 _{inactive} degradation rate	$5 C_s^{-1} h^{-1}$
α_{pi}	Inactive p53 degradation rate	$2 h^{-1}$
α_{mpa}	Mdm2-dependent p53 _{active} degradation rate	$1.4 C_s^{-1} h^{-1}$
α_{wpa}	Wip1-dependent p53 _{active} degradation rate	$0.14 C_s^{-1} h^{-1}$
α_{sm2}	ATR _{active} -dependent Mdm2 inactivation rate	$0.1 C_s^{-1} h^{-1}$
α_m	Mdm2 degradation rate	$1 h^{-1}$
α_w	Wip1 degradation rate	$0.7 h^{-1}$
α_s	ATR _{active} degradation rate	$7.5 h^{-1}$
τ_m	Time delay in Mdm2 production	0.7 h
τ_w	Time delay in Wip1 production	1.25 h
T_s	Signal concentration for half-maximal p53 production	$1 C_s$
n_s	Hill coefficient of active p53 production by ATR _{active}	4
p53 _{inactive0}	Initial p53 _{inactive} concentration	$0.3 C_s$
P53 _{active0}	Initial p53 _{active} concentration	$0 C_s$
Mdm2 ₀	Initial Mdm2 concentration	$0.2 C_s$
Wip1 ₀	Initial Wip1 concentration	$0 C_s$
ATR _{active0}	Initial ATR _{active} concentration	$0 C_s$

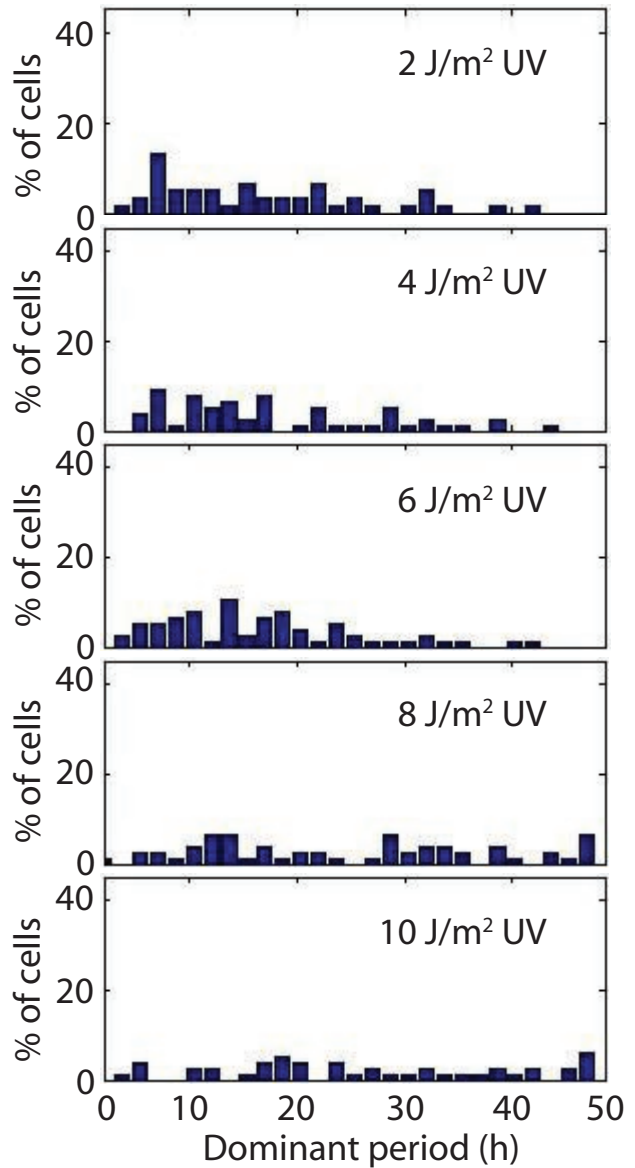
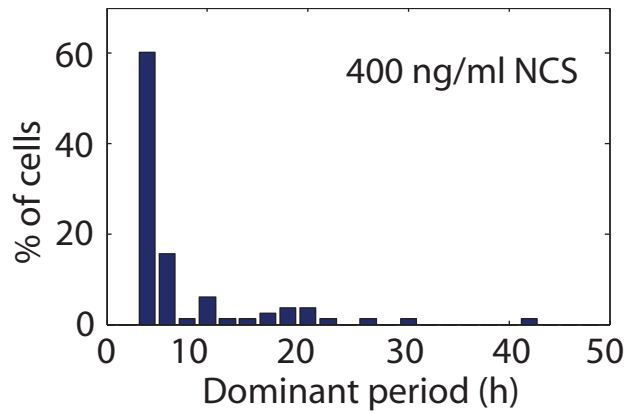
Supplementary Table 1. Parameters and initial conditions of the UV-response model. C_s = simulated concentration units.

Simulated UV dose (J/m ²)	<i>ATR</i> _{active} production rate β_{s2} (C _s h ⁻¹)	Active signaling time t_r (h)
2	2.15	3
4	2.75	5
6	3.45	8
8	4.5	15
10	5.5	23

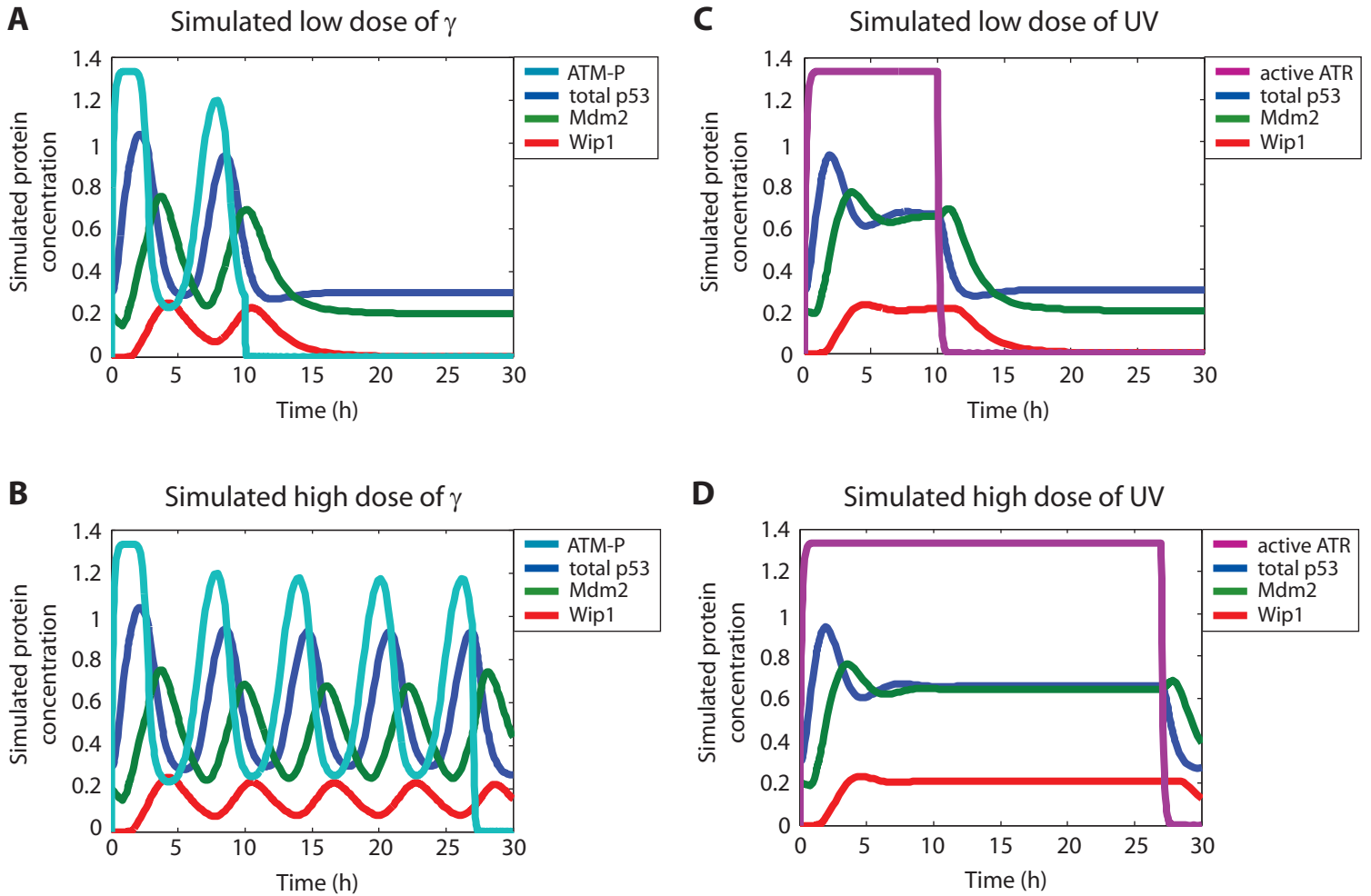
Supplementary Table 2. *ATR*_{active} production rate, β_{s2} , and active *ATR* signaling time, t_r , for each UV dose modeled. C_s = simulated concentration units.

Supplementary Movie 1. p53 response to DSBs. MCF7 cells expressing p53-Venus (pseudocolored green) were treated with 400ng/ml of NCS. Movie duration: 16 hours. Images were taken every 20 minutes.

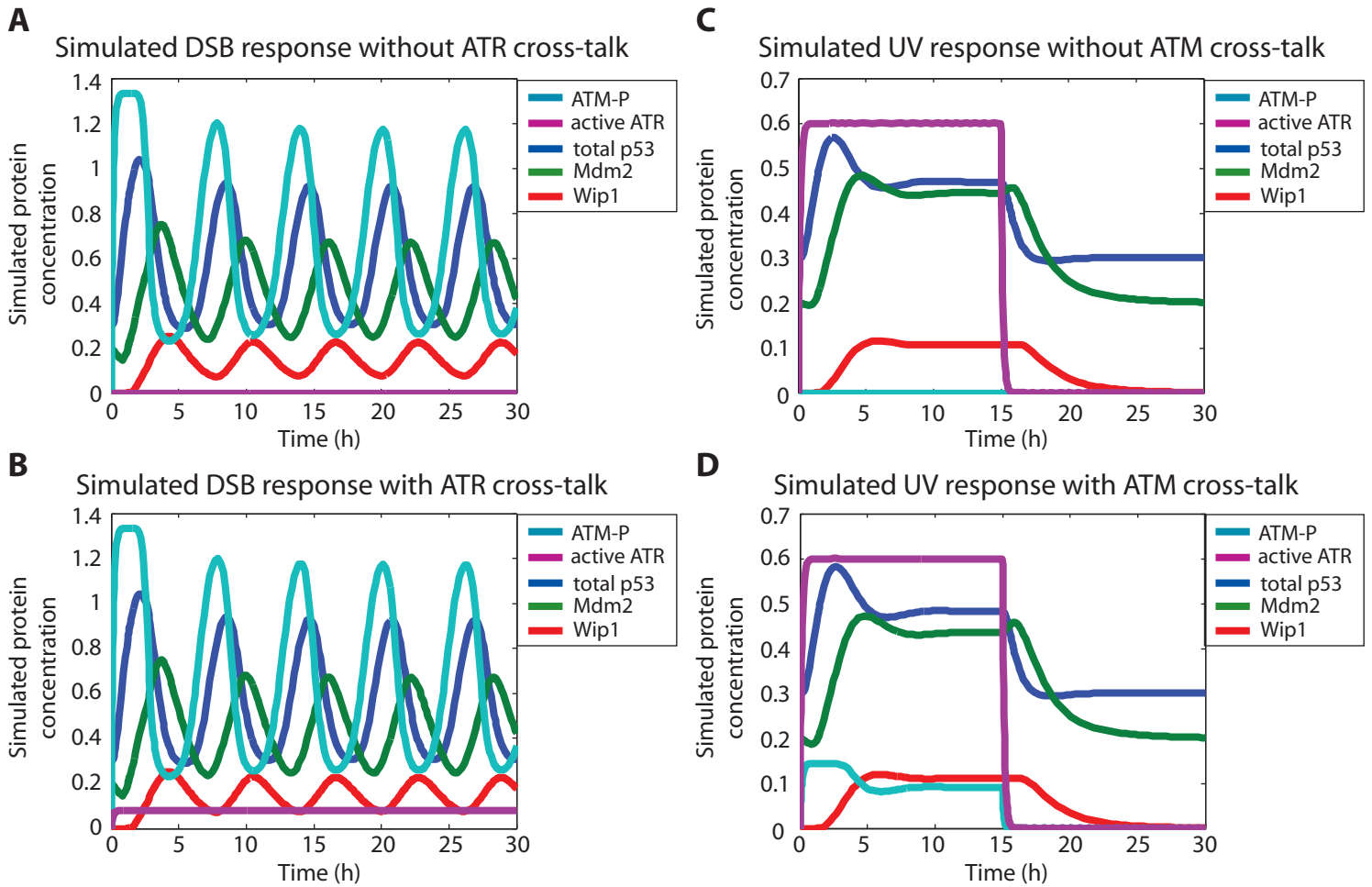
Supplementary Movie 2. p53 response to UV. MCF7 cells expressing p53-Venus (pseudocolored green) were treated with 10 J/m² of UV. Movie duration: 16 hours. Images were taken every 20 minutes.



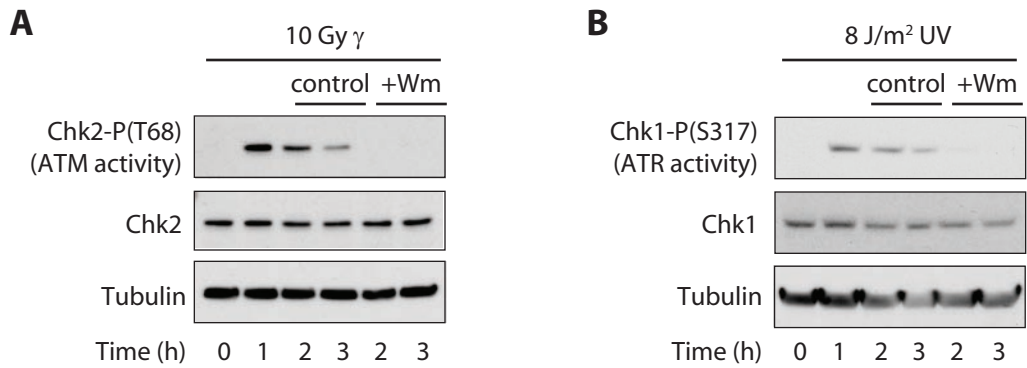
Supplementary Figure 1. Pitch analysis indicates that there is no single characteristic period of p53 pulses in response to UV. Pitch analysis of the traces of p53-Venus in response to 400 ng/ml NCS (left column) or to various doses of UV (right column) was performed as previously described (Geva-Zatorsky et al., 2006).



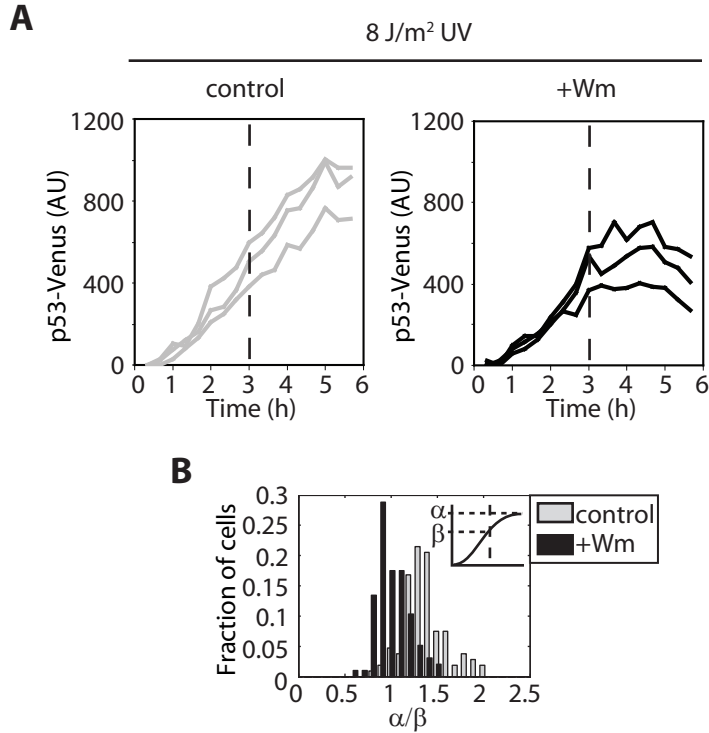
Supplementary Figure 2. Removal of the inhibition of upstream kinase activity by Wip1 eliminates repeated p53 pulses. Simulations of the dynamics of ATM-P, active ATR, p53, Mdm2, and Wip1. All values for parameters are given in (Batchelor et al., 2008) for the γ response (A, B) or Supplementary Table 1 for the UV response (C, D), with $\beta_{s_2} = 10 C_s/h$. The time of repair was simulated at 10 h for low doses of γ (A) and UV (C), and 27 h for high doses of γ (B) and UV (D). Note that the γ dose determines the number of pulses, while the UV dose affects the duration of a single pulse.



Supplementary Figure 3. Cross-talk between ATM and ATR does not qualitatively alter the dynamics of the p53 response to γ and UV. (A, B) Simulations of the dynamics of ATM-P, active ATR, p53, Mdm2, and Wip1 in the absence (A) or presence (B) of cross-talk from the ATR pathway in response to DSBs. (C, D) Simulations of the dynamics of ATM-P, active ATR, p53, Mdm2, and Wip1 in the absence (C) or presence (D) of cross-talk from the ATM pathway in response to 8 J/m² UV. Equations and parameter values for the simulations are given in Supplementary Text and Supplementary Table 1.



Supplementary Figure 4. Wortmannin inhibits ATM and ATR activity. MCF7 cells were irradiated with 10 Gy of γ (A) or 8 J/m² of UV (B). One hour after irradiation, DMSO (control) or 100 μ M of wortmannin (+Wm) were added to the cell medium. Western blot analysis of whole cell lysates was performed to detect levels of phosphorylated Chk2(T68) (A) or phosphorylated Chk1(S317) (B).



Supplementary Figure 5. The p53 response to UV is not excitable even at later times following UV damage. (A) Cells expressing p53-Venus were treated with 8J/m² UV. Three hours after damage, medium containing DMSO (control) or wortmannin (+Wm) was added (dashed line). Representative background-subtracted single cell traces of average p53-Venus intensity are shown for each condition. (B) Histogram of the ratio of p53-Venus intensity at 6h after UV to p53-Venus intensity at time (3h) of DMSO or Wm addition for the experiment shown in (A) (~100 cells/condition).